Journal of Applied Polymer Science

Synthesis of Macroporous Polymer Foams via Pickering High Internal Phase Emulsions for Highly Efficient 2,4,5-Trichlorophenol Removal

Qin Qu, Jianming Pan, Yijie Yin, Runrun Wu, Weidong Shi, Yongsheng Yan, Xiaohui Dai
School of Chemistry and Chemical Engineering, Jiangsu University, Zhenjiang 212013, China
Correspondence to: J. Pan (E-mail: jsdxpjm@126.com)

ABSTRACT: Macroporous polymers foams (MPFs) were prepared by W/O Pickering high internal phase emulsions (HIPEs) stabilized by oleic acid (OA) modified silica nanoparticles (SPs), and then as-prepared MPFs were applied to highly efficient adsorption of 2,4,5-trichlorophenol (TCP). The characterization demonstrated that MPFs possessed macropore (50–150 μm) and interconnected pores (0.5–2 μm), and also had slightly hydrophobic nature (contact angle was 116°) and excellent thermal stability especially bellow 200°C. The influence of pH value, temperature, initial concentration, and contact time for the batch mode adsorption process was investigated, and the results showed that the maximum adsorption capacity and equilibrium time at 25°C were 167.7 mg g^{-1} and 30 min, respectively. Moreover, the experimental data indicate that equilibrium isotherms for TCP fitted to the non-linear Langmuir model, and both the adsorption and desorption kinetics can be represented by the pseudo-second-order model. The possible adsorption mechanism was considered to be the dispersion and hydrophobic interaction, simultaneously. The regeneration of the MPFs for one cycle was 94%. The results above strongly proved that this method reached the effect of highly efficient TCP removal. © 2014 Wiley Periodicals, Inc. J. Appl. Polym. Sci. **2015**, *132*, 41430.

KEYWORDS: adsorption; foams; porous materials

Received 4 June 2014; accepted 20 August 2014
DOI: 10.1002/app.41430

INTRODUCTION

Over the few decades, rapid development of chemical industries had led to a tremendous increase in the use of chlorophenols, such as petroleum refineries, plastics, pharmaceuticals, and pesticide. Acute toxicity of chlorophenols could be resulted in a series of biliousness, including increased respiratory rate, vomiting, and nausea.[1] 2,4,5-Trichlorophenol (TCP) is mainly used as a fungicide in the paper industry and as a precursor in the herbicide industry which has been taken into account as one of the high-priority pollutants due to their toxicity and persistence.[2] Various methods have been suggested for the treatment of drinking water and wastewater containing TCP residues, including biological treatment,[3] photochemical treatment,[4] air stripping and incineration,[5] adsorption technology, and etc.[6] Among these treatment methods, adsorption process is now widely applied as a feasible way because of its low cost, simplicity of operation, and cyclic utilization. In the industry, adsorbents commonly used for adsorptive enrichment of volatile organic compounds included silica gel, activated alumina, activated carbon, and molecular sieve. However, these materials have the disadvantage of small adsorption capacity. The macroporous resin with highly permeability could be considered to be the most promising adsorbents in treating wastewaters containing organic pollutants. Nowadays some studies have illustrated the synthesis and application of macroporous adsorbents for removal of pollutants from waters and wastewaters.[7–9]

At present, high internal phase emulsions (HIPEs) have been considered as the effective approach to synthesize macroporous polymer foams (MPFs). HIPEs are usually defined as internal phase volume fraction greater than 70%,[10] which are dispersed within the continuous. The external (non-droplet) phase was cured and aqueous phase and residual surfactant was removed (in most cases) yielding a highly interconnected macroporous polymers with open cellular structure, so-called polyHIPEs.[11–14] Surfactants, conventional stabilizers, are continuously adsorbed and desorbed at the interface, resulting in a three-dimensionally (3D) interconnected porous structure.[15] However, conventional poly-HIPEs synthesized from surfactant stabilized HIPEs have poor mechanical properties and low permeability despite having open cell structure.[16]

Particles were used to replace surfactants to stabilize the emulsions, the particles-stabilized emulsion was called Pickering

Additional Supporting Information may be found in the online version of this article.

emulsion,[17] which have attracted much interest in recent years. The stability mechanism of the Pickering emulsion system is the solid particles adsorbed at the oil–water surface to prevent droplets of coalescence. Compared to the traditional emulsions, the Pickering emulsions have their excellent advantages: (1) reduces emulsifiers, saves money, reduces our environmental foot print, (2) remarkable stability, not susceptible to conditions, such as pH, salt concentration, temperature, oil phase composition, etc. Therefore, the particles-stabilized emulsions have important research value in the synthesis of porous functional materials. Recently, Ikem et al.[18] successfully synthesized porosity macroporous polymers with a closed-cell pore structure derived from particle-stabilized HIPEs. Ikem et al.[19,20] overcame this disadvantage by using both surfactants and particles as the HIPE emulsifiers and successfully synthesized open porous and highly interconnected poly-Pickering-Pickering Medium internal phase emulsions (MIPEs) having much improved mechanical properties in comparison to conventional poly-HIPEs.

In this study, a synthetic polymer for MPFs was successfully prepared by Pickering emulsion polymerization which was stabilized by the silica particles (SPs) and surfactant (Hypermer 2296). Then TCP was doped to be the target molecule for the further study of the adsorption behavior of as-prepared MPFs.

MATERIALS AND METHODS

Materials

Tetraethyl orthosilicate (TEOS) and TCP were supplied by Aladdin Industrial Corporation (Shanghai, China). Styrene, divinylbenzene (DVB), oleic acid (OA), α,α′-azoisobutyronitrile (AIBN), toluene, methanol, acetone, chloroform, and calcium chloride dihydrate ($CaCl_2{\cdot}2H_2O$) were purchased from Sinopharm Chemical Reagent Co. (Shanghai, China). Ammonium hydroxide (32 wt % $NH_3{\cdot}H_2O$) was purchased from Chemical Reagent Corporation (Shanghai, China). Polyethylene glycol dimethacrylate (PEGDMA) were kindly supplied by Tokyo Chemical Industry Co. All chemicals were of analytical reagent grade. Hypermer 2296 was purchased from CRODA UK.

Instruments

Fourier transmission infrared spectra (FTIR) of MPFs composites were recorded on a Nicolet NEXUS-470 FT-IR apparatus (USA). UV–vis adsorption spectra were obtained with a UV–vis spectrophotometer (UV-2450, Shimadzu, Japan). The morphologies of materials were obtained by scanning electron microscope (SEM, JEOL, JSM-7001F) and transmission electron microscope (TEM, JEOL, JEM-2100). Thermogravimetric analysis (TGA) was carried out using a Differential Scanning Calorimetry (DSC)/Differential Thermal Analysis (DTA)-TG (STA 449C Jupiter, Netzsch, Germany). Contact angle measurement of MPFs was performed on Optical Contact Angle Measuring Device (KSV CM200). The optical micrographs of Pickering HIPEs were collected by a DMM-330C optical microscope equipped with a high performance digital camera (CAIKON, China). Elemental analyzer (FLASH EA1112, Italy) was employed to investigate the elemental composition of MPFs.

Preparation and Surface Modification of SPs (SPs-OA)

About 3.14 mL of aqueous ammonia was firstly dissolved in a mixture of 90 mL ethanol and 10 mL deionized water in a three-neck flask. Then, 6.0 mL of TEOS was added into the above solution and stirred at 25°C for 1.0 h. Then, the obtained SPs were washed with distilled water and methanol, followed by drying under vacuum at 50°C. The stabilized SPs in Pickering system were coated with OA by adsorption process, which was followed Ikem's early work.[18] Briefly, hydrophilic SPs (1.0 g) were immersed in a mixture of chloroform/OA (1 : 2 molar ratio) for 3.0 h using a magnetic stirrer. In order to remove any excess OA from the surface of SPs-OA, SPs-OA were washed with methanol solution prior to drying at 120°C, and kept in a sealed container until use.

Preparation of MPFs

To prepare MPFs, the typical emulsions templates (50 mL) were firstly formed, in which the organic phase consisted of styrene, DVB, and PEGDMA (5 : 4 : 1, vol/vol). Then, the continuous phase of the emulsion templates was further prepared by suspending the SPs-OA into organic phase. AIBN (1.0 mol %, with respect to the monomers) was dissolved in the suspension under gentle stirring at 400 rpm. About 35 mL of internal aqueous phase containing $CaCl_2{\cdot}2H_2O$ (0.27*M*) were added dropwise under constant agitation for 2.0 min. Finally, emulsion templates were formed by later adding 0.75 mL of Hypermer 2296 to co-stable Pickering-emulsions under continued stirring for 30 s. W/O Pickering HIPEs stabilized by SPs-OA and Hypermer 2296 were transferred into an ampere bottle and polymerized at 70°C for 24 h. To remove the unreacted monomer and the excess surfactant, the obtained crude MPFs were purified by soxhlet extraction with methanol-acetic acid solution ($V : V = 9 : 1$). After eluting, MPFs were dried in the oven at 120°C to constant weight.

Adsorption Experiments

In batch pH studies, the MPFs (0.01 g) were suspended in 10 mL of TCP solution (100 mg L^{-1}) with the pH range of 2.0–9.0, respectively. The testing solutions were kept at 25°C for 12 h, and then were filtered and the final pH was measured.

In the determination of equilibrium adsorption isotherm, 0.01 g of MPFs were added into 10 mL of TCP solution (pH = 6.0) of different initial concentrations ranging from 10 mg L^{-1} to 400 mg L^{-1}, and temperature of solution was maintained at 25°C, 35°C, and 45°C for 12 h, respectively. Moreover, the equilibrium adsorption capacity (Q_e, mg L^{-1}) was calculated by eq. (1):

$$Q_e = \frac{(C_0 - C_e)V}{W} \quad (1)$$

where C_0 (mg L^{-1}) and C_e (mg L^{-1}) are initial and equilibrium TCP concentrations, respectively. V (mL) and W (g) are the solution volume and the adsorbent weight, respectively.

In the adsorption kinetic experiments, 0.01 g of MPFs and 10 mL of TCP solutions (100 mg L^{-1}) were maintained at a constant pH = 6.0 at 25°C for different contact times (10–480 min). After the desired contact time, the dispersions were centrifuged and the MPFs were removed. The amount of adsorption at time t (min), Q_t (mg g^{-1}), was calculated by eq. (2):

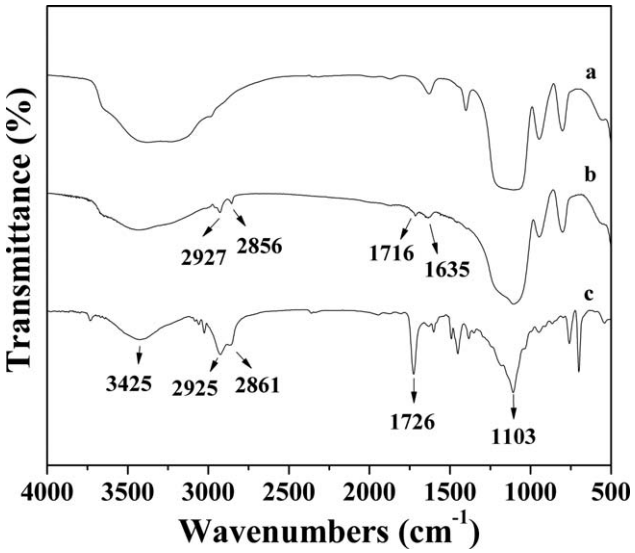

Figure 1. FTIR spectra of SPs (a), SPs-OA (b), and MPFs (c).

$$Q_t = \frac{(C_0 - C_t)V}{W} \quad (2)$$

where C_t (mg L^{-1}) is the liquid-phase concentrations of TCP at time *t*.

Desorption Experiments

In order to estimate the reversibility of TCP adsorption, adsorption–desorption process was carried out. Adsorption experiment was firstly conducted using 10 mg of the Macroporous Polymer Foams (MPFs) with 10 mL solution containing 100 mg L^{-1} TCP at 25°C for 12 h. Then saturated MPFs was separated from the solution and added into a 10-mL test tube, using 50% ethanol solutions (methanol : H_2O) as eluent for desorption of the TCP at 298 K for different contact times (10–480) min. Finally, the dispersions were centrifuged after each time of contact and the concentration of TCP in liquid phase was determined. The percent desorption ratio was obtained from eq. (3):

$$\text{Desorption } (\%) = \frac{C_{de}}{C_{ad}} \times 100 \quad (3)$$

where C_{de} (mg L^{-1}) and C_{ad} (mg L^{-1}) are the concentrations of TCP desorbed and adsorbed in adsorption–desorption process, respectively.

RESULTS AND DISCUSSION

Characterization

The FTIR spectra of SPs (a), SPs-OA (b), and MPFs (c) are shown in Figure 1. The band at 1103 cm^{-1} was attributed to the stretching mode of Si—O. Compared with SPs, the new peaks at 1716 cm^{-1} of SPs-OA were assigned to C═O stretching vibrations, and the vibration bands at 2927 cm^{-1} and 2856 cm^{-1} for SPs-OA were assigned to the C—H asymmetry stretching vibrations of —CH_3 and —CH_2 groups,[21] indicating the presence of OA on the surface of SPs by modification. The MPFs showed a significant peak at 1726 cm^{-1}, which was assigned to C═O stretching vibrations of PEGDMA, and the typical absorption at 2925 cm^{-1} and 2861 cm^{-1} were attributed to the C—H asymmetry stretching vibrations of both —CH_3 and —CH_2 groups, and the bands at 3425 cm^{-1} and 1635 cm^{-1} of the MPFs may result from the stretching vibration of O—H bonds of silanol groups and bending vibrations of adsorbed water on the surface of SPs, respectively. The results of elemental analysis are shown in Supporting Information Table S1, which was 68.77% and 7.37% for C and H, respectively. Thereby, the high amount of C suggested that the MPFs were successfully introduced onto the surface of SPs-OA.

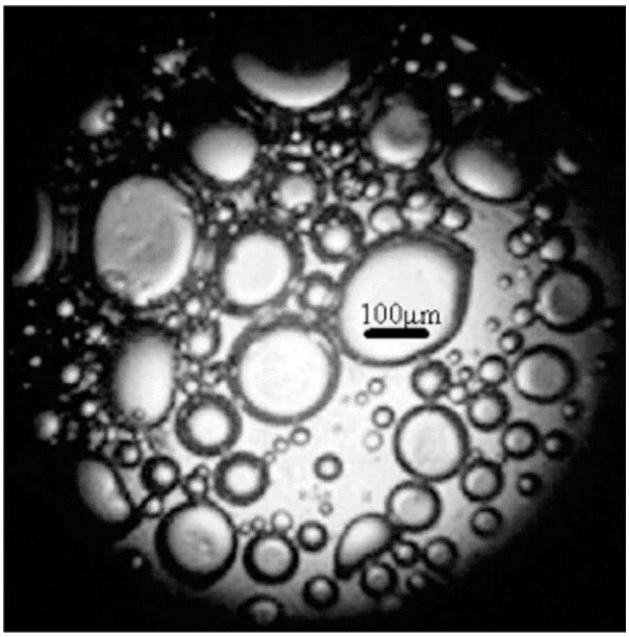

Figure 2. Optical microscopic images of Pickering HIPEs stabilized by SPs, the scale bars present 100 μm.

The Pickering HIPEs were observed by optical microscopy which is shown in Figure 2. The average diameters as well as the size distributions were studied. As shown in Figure 2, the size of the droplets ranged from 50 to 100 μm, and the size distributions were relatively wide, indicating the formation of a stable Pickering HIPEs system. The micromorphology of the

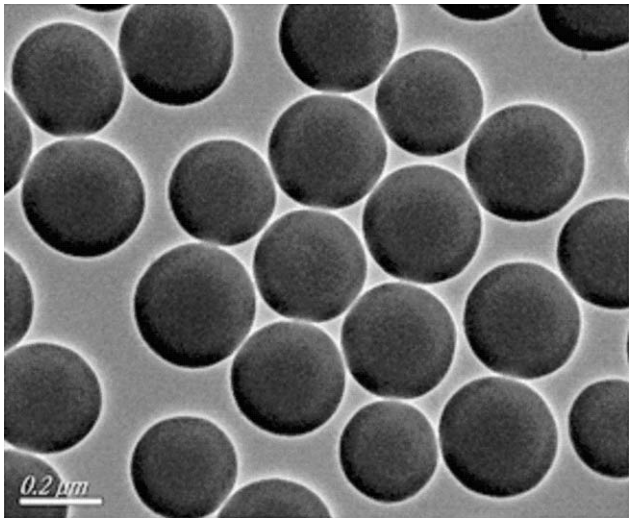

Figure 3. The micromorphology of the SPs.

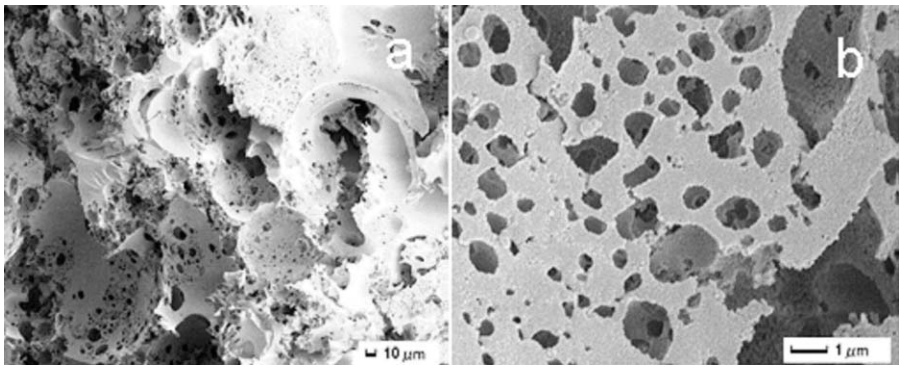

Figure 4. SEM images of MPFs (a) and their amplified images (b).

SPs was examined by TEM, and the micrographs are shown in Figure 3. In Figure 3, it was observed that SPs had an average size of 200 nm. The morphology of MPFs was examined by SEM, and the results are presented in Figure 4. It was seen that macroporous voids (50–150 μm) were connected by interconnected pores (0.5–4 μm) which enable fast mass transfer by convection rather than diffusion.[22] Moreover, many intercrosslinked pores were distributed in macroporous voids, suggesting the excellent permeability.[16] Furthermore, the size of emulsion droplets was similar to the pores, illustrating that Pickering HIPEs was stable and no destabilization occurred during the polymerization.

TGA curves of the SiO_2, SPs-OA, and MPFs are shown in Figure 5. According to the results of SiO_2 and SPs-OA, the OA content of SPs-OA was determined to be 2.97 wt %. All in all, it was also demonstrated that the OA was successfully introduced onto the surface of the SPs. In addition, the weight losses of 1.41 wt % for MPFs were observed up to 142°C, which can be attributed to the loss of free interlayer water. The TGA curve of MPFs showed that a significant weight loss of 85.72 wt % ranged from 142°C to 462°C, which was attributed to the structural dehydroxylation.

Figure 6 illustrates the contact angle for MPFs contact with water from optical contact angle measuring device. The prepared MPFs were moderate hydrophobic, which was indicated from the corresponding contact angle showing a numerical value of 116°. Due to our adsorption system of which the adsorbents were suspended in a liquid environment, it can be assumed that the slightly hydrophobic nature of the MPFs should enhance the adsorption efficiency.

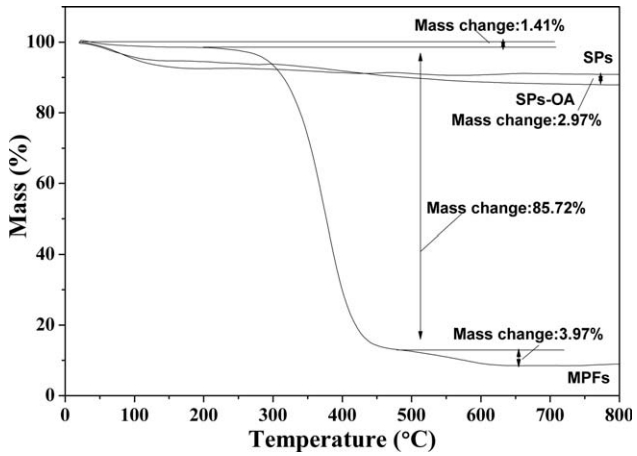

Figure 5. The TGA curves of SPs, SPs-OA, and MPFs.

Effect of the Solution pH

The solution pH value plays an important role in adsorption uptake. To study the influence of the pH on the adsorption capacity of MPFs, the pH of solution was varied from 2.0 to 10 in the batch mode experiments. The effect of initial pH on equilibrium pH and effect of pH solution on the adsorption of TCP on the MPFs are illustrated in Figure 7(a,b), respectively. It was observed that adsorption of neutral TCP at pH = 2.0, 3.0, and 8.0 didn't cause any significant change in equilibrium pH [Figure 7(a)]. The final pH was generally higher than the initial pH before pH 8.0 in the blank, whereas it was lower at pH = 9.0 and 10. From Figure 7(b), the adsorption uptake of MPFs composites decreased with increasing initial pH at pH $\geq$ 3, and decreased rapidly over pH of 6.0, which achieved the maximum value at pH = 3 for TCP. The result was related to the surface charge of adsorbent and the degree of ionization

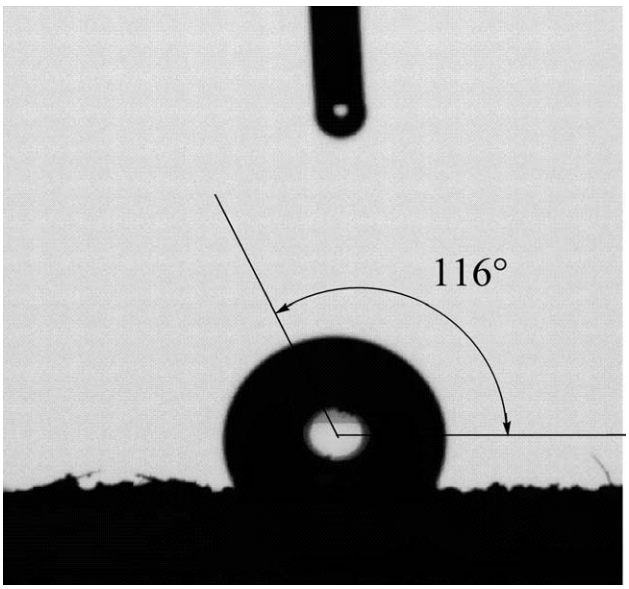

Figure 6. Contact angle of MPFs.

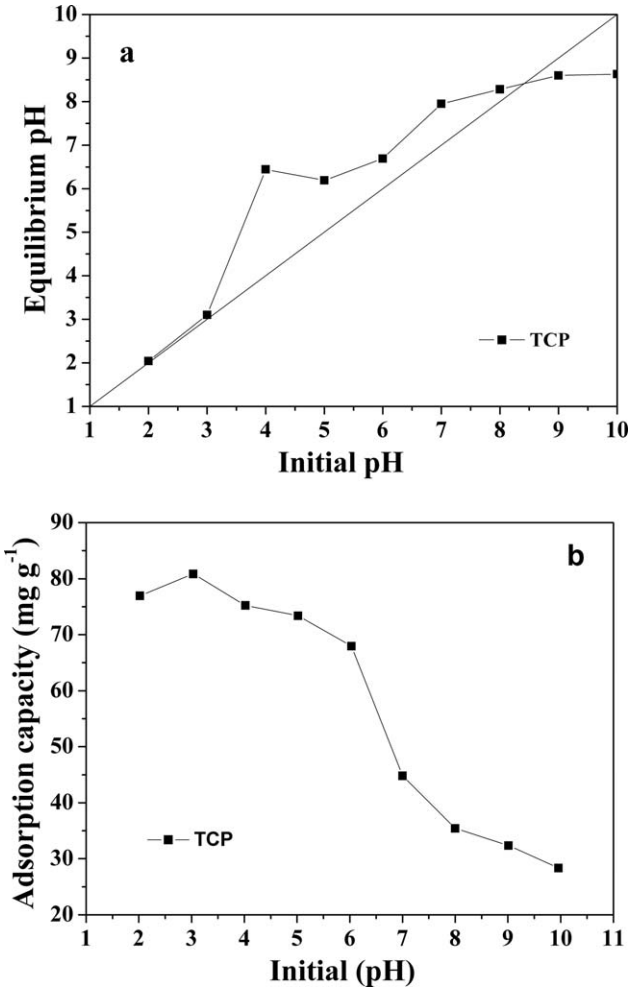

Figure 7. Effect of initial pH on equilibrium pH (a) and Effect of pH on adsorptive removal of TCP (b). Temperature: 298 K, adsorbent dose: 0.01 g, solution volume: 10 mL, and contact time: 12 h.

of adsorbate. When pH < 7 ($pK_{a\text{TCP}} = 6.8$), the degree of unionized TCP molecules were high and decreased with increasing pH, the total surface charge of MPFs composite would be on average positive, and the electrostatic attractive forces and hydrophobic interaction do favor to the neutral TCP molecules onto adsorbent surface. However, when pH > 7, the degree of ionized TCP molecules were higher than the unionized TCP, the adsorption capacity was lower due to the electrostatic repulsions.[23] pH = 6.0 was adopted to investigate the adsorption properties which was closed to the value of the environment system.

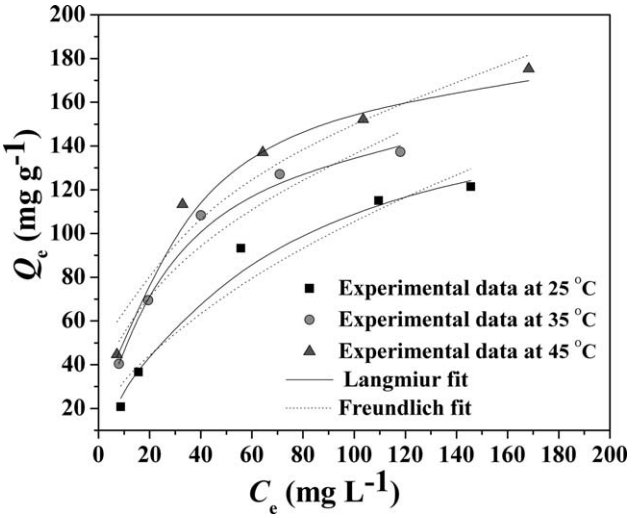

Figure 8. Comparison of Langmuir and Freundlich isotherm models for TCP using nonlinear regression. Adsorbent dose: 0.01 g, solution volume: 10 mL, contact time: 12 h, and solution pH: 6.0 for TCP.

Adsorption Isotherm

In order to study the adsorption system for the adsorption of TCP from solution, it is vital to establish the equilibrium properties of the adsorption process by an appropriate coefficient (R^2). Consequently, the equilibrium data of TCP were fitted to the Langmuir[24] and Freundlich[25] isotherm models presented in Figure 8. The linear and nonlinear forms of Langmuir isotherm model are expressed by the following equations, respectively:

$$\frac{C_e}{Q_e} = \frac{1}{Q_m K_L} + \frac{C_e}{Q_m} \quad (4)$$

$$Q_e = \frac{K_L Q_m C_e}{1 + K_L C_e} \quad (5)$$

where Q_e (mg L^{-1}) is the equilibrium adsorption capacity, C_e (mg L^{-1}) is the equilibrium concentration of adsorbate at equilibrium, and Q_m (mg L^{-1}) is the maximum adsorption capacity

Table I. Adsorption of Isotherm Constants for TCP

		TCP		
Adsorption isotherm models	Constants	298 K	318 K	338 K
	R^2	0.990	0.996	0.990
Langmuir equation	Q_m (mg g^{-1})	167.7	170.6	195.2
	K_L (L mg^{-1})	0.020	0.039	0.040
	R_L	0.145	0.158	0.130
	R^2	0.938	0.918	0.940
Freundlich equation	K_F (L mg^{-1})	9.890	22.36	29.71
	1/n	0.516	0.394	0.353

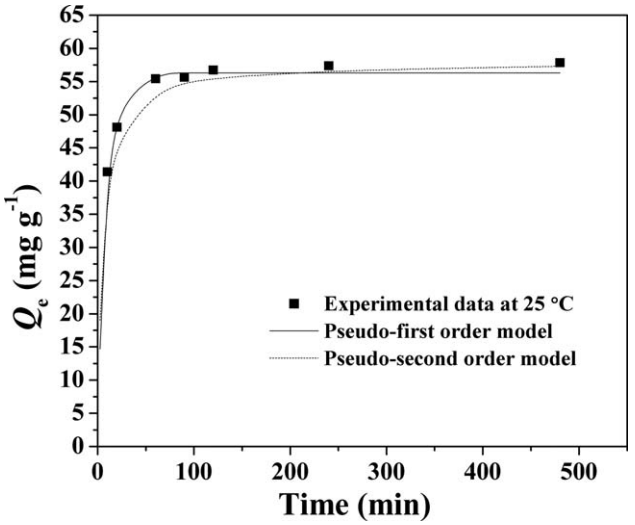

Figure 9. Kinetic data for the adsorption of TCP onto MPFs (a). Temperature: 25°C, adsorbent dose: 0.01 g, solution volume: 10 mL, and solution pH: 6.0 for TCP.

of the adsorbent. K_L (L mg^{-1}) is the Langmuir adsorption constant.

For predicting the favorability of an adsorption system, the Langmuir equation can also be expressed in terms of a dimensionless separation factor R_L defined as follows[24]:

$$R_L = \frac{1}{1 + C_m K_L} \quad (6)$$

where C_m is the maximal initial concentration of adsorbate. The R_L indicates the favorability and the capacity of adsorption system. When $0 < R_L < 1.0$, it represents good adsorption.

The linear and nonlinear forms of Freundlich isotherm model are expressed by the following equations, respectively:

$$\ln Q_e = \ln K_F + \frac{1}{n} \ln C_e \quad (7)$$

$$Q_e = K_F C_e^{\frac{1}{n}} \quad (8)$$

K_F (mg L^{-1}) is the Freundlich adsorption equilibrium constant, and $1/n$ is a measure of exchange intensity or surface heterogeneity, with a value of $1/n$ smaller than 1.0 describing favorable removal conditions.[26]

The adsorbed TCP quantity increased from 6.85 to 215.4 mg L^{-1} with the increasing of initial TCP concentration. When the temperature was varied from 25°C to 45°C, the maximum adsorption capacity of TCP increased from 167.7 to 195.2 mg L^{-1} (Table I). As a comparison, the Langmuir and Freundlich isotherm models for TCP at 25°C, 35°C, and 45°C are shown in Figure 8, and adsorption of isotherm constants for TCP are listed in Table I. From Table I, it was concluded that the correlation coefficients ($R^2 = 0.990$–0.996) of Langmuir model fitted better than the Freundlich ($R^2 = 0.918$–0.940), suggesting that TCP adsorption on the surface of the MPFs was a surface with homogeneous binding sites[27] and monolayer coverage.[6,28] It can also be seen that the values of $1/n$ and R_L were all less than 1.0, indicating that adsorption TCP was favorable. In Figure 8, it can also be observed that the adsorption curve was sharply increased at the low concentration and become smoother at higher concentration (100 mg L^{-1}). This may account for high concentration and higher affinity to the TCP molecules. This phenomenon indicated that increasing initial concentration was valuable to the adsorption.

Adsorption Kinetics

In order to examine the influence of contact time on the adsorption capacity of MPFs, both the pseudo-first-order and pseudo-second-order models were fitted to experimental data. The kinetic models of effective contact time are shown in Figure 9. The pseudo-first-order equation can be expressed as linear and nonlinear forms by eqs. (9) and (10), respectively:

$$\ln (Q_e - Q_t) = \ln Q_e - k_1 t \quad (9)$$

$$Q_t = Q_e - Q_e e^{-k_1 t} \quad (10)$$

Table II. Kinetic Constants for the Adsorption of TCP Onto PFMs Pseudo-First-Order Equation and Pseudo-Second-Order Equation and Elovich Equation

$Q_{e,exp}$ (mg g^{-1})	Pseudo-first-order equation		Pseudo-second-order equation		Elovich equation	
	$Q_{e,exp}$ (mg g^{-1})	56.29	$Q_{e,c}$ (mg g^{-1})	57.28	α (g^{-1} mg^{-1} min)	18,891
57.82	k_1 (L min^{-1})	0.1210	k_2 ($\times 10^{-3}$ g mg^{-1} min^{-1})	4.113	β (g^{-1} mg)	0.2396
	R^2	0.9019	R^2	0.9957	R^2	0.8360

Table III. Kinetic Constants for the Desorption of TCP onto PFMs Pseudo-First-Order Equation and Pseudo-Second-Order Equation and Elovich Equation

$Q_{e,exp}$ (mg g^{-1})	Pseudo-first-order equation		Pseudo-second-order equation		Elovich equation	
	$Q_{e,exp}$ (mg g^{-1})	52.30	$Q_{e,c}$ (mg g^{-1})	55.09	α (g^{-1} mg^{-1} min)	15,160
55.45	k_1 (L min^{-1})	0.1255	k_2 ($\times 10^{-3}$ g mg^{-1} min^{-1})	4.404	β (g^{-1} mg)	0.2987
	R^2	0.6640	R^2	0.9730	R^2	0.8790

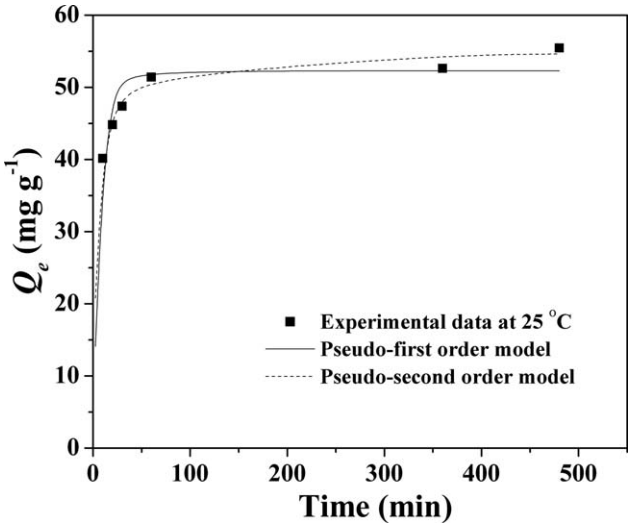

Figure 10. Kinetic data for the desorption of TCP onto MPFs (a). Temperature: 25°C, adsorbent dose: 0.01 g, solution volume: 10 mL, and solution pH: 6.0 for TCP.

The pseudo-second-order equation can be expressed as linear and nonlinear forms by eqs. (11) and (12), respectively:

$$\frac{t}{Q_t} = \frac{1}{k_2 Q_e^2} - \frac{t}{Q_e} \tag{11}$$

$$Q_t = \frac{k_2 Q_e^2 t}{1 + k_2 Q_e t} \tag{12}$$

The Elovich equation is expressed by eq. (13):

$$Q_t = \frac{1}{\beta}\ln(\alpha\beta) + \frac{1}{\beta}\ln t \tag{13}$$

Q_t (mg L^{-1}) and Q_e (mg L^{-1}) are the amount of TCP adsorbed at time t and at equilibrium, respectively. k_1 (L min^{-1}) and k_2 (g mg^{-1} min^{-1}) are rate constants of the pseudo-first-order and pseudo-second-order models, which can be calculated from the plots of $\ln(Q_e - Q_t)$ versus t and t/Q_t versus t, respectively. α is the initial adsorption rate (mg g^{-1} min^{-1}), β is related to the extent of surface coverage and the activation energy for chemisorption (g mg^{-1}). A plot of Q_t versus $\ln t$ gives a linear trace with a slope of $(1/\beta)$ and an intercept of $1/\beta \ln(\alpha\beta)$.

The kinetic constants for the adsorption of TCP onto MPFs by pseudo-first-order equation and pseudo-second-order equation are summarized in Table II. The pseudo-second-order kinetic model ($R^2 = 0.9957$) yielded a better fit than the pseudo-first-order model ($R^2 = 0.9019$) and Elovich equation ($R^2 = 0.8360$) for the adsorption of TCP onto MPFs. It was considered that the chemical process could be the rate-limiting step in the adsorption process for TCP.[6,28]

Figure 9 revealed that the adsorption curve was sharply increased at the beginning of adsorption and then steady and saturation levels were gradually reached within 30 min for TCP. This result was interesting because equilibrium time was one of the important parameters for economical wastewater treatment applications. This observation could be explained by intraparticle diffusion, initially the adsorbate molecules had to first encounter the boundary layer effect and then diffused onto the adsorbent

Table IV. Thermodynamic Parameters of TCP Adsorption on MPFs

C_0 (mg g^{-1})	T (K)	$\Delta H°$ (kJ mol^{-1})	$\Delta S°$ (J mol^{-1})	$\Delta G°$ (kJ mol^{-1})	R^2
	298			−0.5076	
100	308	12.06	42.19	−0.9294	0.979
	318			−1.3513	

Table V. The Comparison of the Maximum Monolayer Adsorption Capacity of Various Chlorophenols on Various Adsorbents

Adsorbent	T (K)	Q_{max} (mg g−1)	W (mg)	V (mL)	C_0 (mg g−1)	pH	Equilibrium time (min)	Adsorbate	References
Activated carbon prepared from coconut shell	303	122.336	500	100	50	2	-	2,4,6-TCP	29
Activated carbon of commercial grade	303	112.35	700	100	50	2	-	2,4,6-TCP	29
Acid-activated montmorillonite	288	35	20	50	100	4	20	TCP	30
activated clay	303	123.46	400	200	30-220	4	30-40	2,4,6-TCP	6
surfactant-modified bentonite	303	13.9	100	50	10-400	3	30	2,4,6-TCP	31
activated carbon prepared from oil palm empty fruit bunch	303	168.89	100	100	200	-	-	2,4,6-TCP	32
MPFs	298	167.5	10	10	100	6	30	TCP	Our work

surface and then finally entered the pores to reach to internal surface.[29] This phenomenon took relatively longer contact time.

Desorption and Reuse

The kinetic constants for desorption of TCP onto MPFs by pseudo-first-order equation and pseudo-second-order equation and Elovich equation are summarized in Table III.

It cost 30 min to achieve the desorption equilibrium in Figure 10. For the studied samples, slow desorption was predominant throughout the whole procedure. Contribution of rapid desorption was relatively high in the early stage, then gradually decreased and ultimately became negligible fraction after 1.0 h. On the whole, the pattern of desorption was similar with adsorption. As further compared with our adsorption results on adsorption kinetics using the same samples, the rate constant of rapid desorption were greater than those in adsorption. The regeneration of the MPFs for one cycle was 94% at pH = 6.0, indicating that the prepared MPFs can be repeatedly reused.

Adsorption Thermodynamics

In order to define whether the adsorption process is endothermic or exothermic and spontaneous, the thermodynamic parameters (ΔH^o, ΔS^o, and ΔG^o) for TCP adsorption on MPFs were used to calculate the temperature dependence on adsorption isotherms. The standard enthalpy change (ΔH^o) and the standard entropy (ΔS^o) are then calculated from the linear plot of lnK^o versus1/T for TCP adsorption on the MPFs by eq. (14):

$$\ln K^o = \frac{\Delta S^o}{R} - \frac{\Delta H^o}{RT} \tag{14}$$

where R is the universal gas constant (8.314 J mol^{-1} K^{-1}), T is the temperature in Kelvin. K^o is the adsorption equilibrium constant.

The standard free energy change ΔG^o can be calculated by eq. (15):

$$\Delta G^o = \Delta H^o - T\Delta S^o \tag{15}$$

The thermodynamic parameters of TCP adsorption on MPFs are listed in Table IV. The positive ΔH^o value suggested that TCP adsorption on the surface of the MPFs was an endothermic procedure. The negative ΔG^o values increased with the temperature (from 298 K to 318 K), indicating that the adsorption of TCP on the MPFs was a spontaneous process. Thus, rising temperature was beneficial to the TCP adsorption.

Comparison with Other Work

Table V listed the comparison of the maximum monolayer adsorption capacity of various types of chlorophenols on various adsorbents.[6,30–34] The MPFs prepared in this work showed relatively larger TCP adsorption capacity of 167.7 mg g^{-1}, as compared to some previous works[6,30–34] reported in the literature, suggesting the prepared MPFs were very suitable and effective for TCP cleanup.

CONCLUSIONS

It was demonstrated the MPFs can be successfully synthesized via W/O particle-stabilized HIPEs and were carefully investigated to remove the TCP from aqueous solution. It was expected that the effective TCP removal shows high levels of adsorption toward TCP which depend on the pH value, contact time, and temperature. Thermodynamic parameters of TCP adsorption on MPFs indicate that the TCP adsorption was a spontaneous endothermic procedure. Thereby, the prepared MPFs were expected to clean up the poisonous and harmful materials including TCP, fast and efficient in practical applications.

ACKNOWLEDGMENTS

This work was financially supported by the National Natural Science Foundation of China (No. 21107037, No. 21176107), Natural Science Foundation of Jiangsu Province (No. BK2011461, No. BK2011514), National Postdoctoral Science Foundation (No.2013M530240), Postdoctoral Science Foundation funded Project of Jiangsu Province (No. 1202002B) and Programs of Senior Talent Foundation of Jiangsu University (No. 12JDG090).

REFERENCES

1. Fawell, J. K.; Hunt, S. Environmental Toxicology: Organic Pollutants, 1st ed.; Ellis Horwood: England, **1998**.
2. Field, A. J.; Sierra-Alvarez, R. *Rev. Environ. Sci. Biotechnol.* **2008**, *7*, 211.
3. Dilaver, M.; Kargi, F. *Bioresour. Technol.* **2009**, *100*, 1459.
4. Poulopoulos, S. G.; Nikolaki, M.; Karampetsos, D.; Philippopoulos, C. J. *J. Hazard. Mater.* **2008**, *153*, 582.
5. Rengaraj, S.; Li, X. Z. *J. Mol. Catal. A: Chem.* **2006**, *243*, 60.
6. Hameed, B. H. *Colloids Surf. A* **2007**, *307*, 45.
7. Richarda, D.; Núnez, M. L. D.; Schweich, D. *Chem. Eng. J.* **2009**, *148*, 1.
8. Nemr, A. E.; Ola, A.; Amany, E. S.; Azza, K. *J. Hazard. Mater.* **2009**, *161*, 102.
9. Sanchez-Martin, M. J.; Rodriguez-Cruz, M. S.; Andrades, M. S.; Sanchez-Camazano, M. *Appl. Clay Sci.* **2006**, *31*, 216.
10. Lissant, K. J. *J. Colloid Interface* **1966**, *22*, 462.
11. Menner, A.; Powell, R.; Bismarck, A. *Macromolecules* **2006**, *39*, 2034.
12. Barbetta, A.; Cameron, N. R.; Cooper, S. J. *Chem. Commun.* **2000**, *3*, 221.
13. Cameron, N. R. *Polymer* **2005**, *5*, 1439.
14. Kimmins, S. D.; Cameron, N. R. *Adv. Funct. Mater.* **2011**, *21*, 211.
15. Pulko, I.; Kolar, M.; Krajnc, P. *Sci. Total Environ.* **2007**, *386*, 114.
16. Manley, S. S.; Graeber, N.; Grof, Z.; Menner, A.; Hewitt, G. F.; Stepanek, F.; Bismarck, A. *Soft Matter* **2009**, *5*, 4780.
17. Pickering, S. U. *J. Chem. Soc. Trans.* **1907**, *91*, 2001.
18. Ikem, V. O.; Menner, A.; Bismarck, A. *Langmuir* **2010**, *26*, 8836.
19. Ikem, V. O.; Menner, A.; Horozov, T. S.; Bismarck, A. *Adv. Mater.* **2010**, *22*, 3588.
20. Ikem, V. O.; Menner, A.; Bismarc, A. *Soft Matter* **2011**, *7*, 6571.

21. Garbassi, F.; Balducci, L.; Chiurlo, P.; Deiana, L. *Appl. Surf. Sci.* **1995**, *84*, 145.
22. Pulko, I.; Wall, J.; Krajnc, P.; Cameron, N. R. *Chem.—Eur. J.* **2010**, *16*, 2350.
23. Zaghouane-Boudiaf, H.; Boutahala, M. *Chem. Eng. J.*, **2011**, *170*, 120.
24. Mazzotti, M. *J. Chromatogr. A* **2006**, *1126*, 311.
25. Allen, S. J.; Mckay, G.; Porter, J. F. *J. Colloid Interface Sci.* **2004**, *280*, 322.
26. Li, K. Q.; Wang, X. H. *Bioresour. Technol.* **2009**, *100*, 2810.
27. Gupta, V. K.; Rastogi, A.; Nayak, A. *J. Colloid Interface Sci.* **2010**, *342*, 533.
28. Theivarasu, C.; Mylsamy, S. *Int. J. Eng. Sci. Technol.* **2010**, *2*, 6284.
29. Faust, D. S.; Aly, M. O. Chemistry of Wastewater Treatment; Butterworths: Boston, **1983**.
30. Radhika, M.; Palanivelu, K. *J. Hazard. Mater. B* **2006**, *138*, 116.
31. Zaghouane-Boudiaf, H.; Boutahala, M. *Int. J. Miner. Process.* **2011**, *100*, 72.
32. Anirudhan, T. S.; Ramachandran, M. *J. Water Process Eng.* **2014**, *1*, 46.
33. Hameed, B. H.; Tan, I. A. W.; Ahmad, A. L. J. *Hazard. Mater.* **2009**, *164*, 1316.